Few-layer-graphene/polycarbonate nanocomposites as dielectric and conducting material

P. K. Sain,[1] R. K. Goyal,[2] Y. V. S. S. Prasad,[1] Jyoti,[3] K. B. Sharma,[4] A. K. Bhargava[1]

[1]Department of Metallurgical and Materials Engineering, Malaviya National Institute of Technology Jaipur, India
[2]Department of Metallurgy and Materials Science, College of Engineering Pune, India
[3]Department of Physics, University of Rajasthan, Jaipur, India
[4]Department of Physics, SS Jain Subodh PG College, Jaipur, India
Correspondence to: P. K. Sain (E-mail: pkspmt@gmail.com) and R. K. Goyal (E-mail: rkgoyal72@yahoo.co.in)

ABSTRACT: An attempt is taken to develop a flexible and light weight polycarbonate-based nanocomposite system which could be successfully used as a dielectric material below percolation and as conducting material beyond percolation. The nanocomposite system has been prepared by solution mixing method in which few layer graphene was incorporated as conductive filler. X-ray diffractometry, Raman spectroscopy, transmission electron microscopy, scanning electron microscopy techniques were employed for characterization studies. The dielectric constant and conductivity were evaluated using precision impedance analyzer. Percolation threshold has been observed to occur at 3.5 wt % of few layer graphene. Dielectric constant of the nanocomposite system, in the smearing region, has been found to increase from ~3.3 (without filler) to ~70 (at 5 wt % FLG) with a dissipation factor of 0.07. The conductivity of the system was increased from 10^{-9} S/cm without FLG to 10^{-2} S/cm with 7 wt % of few layer graphene. © 2015 Wiley Periodicals, Inc. J. Appl. Polym. Sci. **2015**, *132*, 42443.

INTRODUCTION

Increasing possibilities for use of polymer-based composite materials in different electronic applications stimulated the research in developing polymeric composite materials those could be used as dielectric material or as conducting material. Generally, the polymers are regarded as insulating materials having dielectric constant below 10 and very low electrical conductivity (10^{-12} S/cm or less). However, the polymer's dielectric constant and conductivity have been improved by impregnating them with different types of fillers.[1–7] Goyal et al.[8,9] studied the electronic properties of polyphenylene sulphide/ graphite, and polyvinyl chloride (PVC)/Copper (Cu) composites. Based on these studies, they suggested their uses in electrostatic dissipation (ESD) and electromagnetic interference (EMI) shielding applications. Wong et al.[10] studied the dielectric properties of conducting filler-polymer composite systems. Some studies have shown that when conducting filler (metal particles, metal fibers, carbon black, carbon nanotubes, etc.) is added in insulating matrices then, at a certain amount of filler, the conductivity increases abruptly.[11–15] The concentration at which the abrupt increase in conductivity on-sets is regarded as percolation threshold and this phenomenon is called percolation. Percola-tion occurs in such type of composites due to the formation of three dimensional paths for charge carriers which may be due to the physical connections between the conductive fillers or may be due to the tunnelling of charge carriers.[16,17] The perco-lation (abrupt increase in conductivity) has been found to occur within a narrow range of filler concentration and this range is termed as smearing region. Researchers also reported the abrupt increment in dielectric constant within the smearing range near percolation.[18,19] The challenges in developing such polymeric materials for practical realization are to maintain flexibility, developing high dielectric constant coupled with low dissipation factor or conductivity at low concentration of filler, and easy processabilty at end use application. Polymer composites embedded with high aspect ratio fillers have been found to exhibit percolation at very low filler concentration.[20,21] For instance, Moreno et al.[21] achieved the percolation in silver nanowires/polycarbonate system at only 0.04 wt % of silver nanowire having aspect ratio of 85. The size of the conducting filler also a crucial factor in achieving percolation, for instance, Boudenne et al.[22] achieved percolation in polypropylene (PP) at lower concentration with smaller size than that with larger size

of same copper filler (particles shape was not perfectly spherical). The matrix polymer also affects the percolation in polymer composites. Carmona[11] showed the percolation dependency on the matrix polymer (LPE, PS, PMMA, Nylon 6, etc.) with the same carbon black filler, but the reason was not clearly mentioned. So, there are many factors which control the percolation in such heterogeneous systems. In such percolative polymeric composites, the dielectric constant can be increased considerably in the smearing range. Hence, the development of dielectric materials with such conductive filler filled polymer composite system is tedious due to very narrow smearing range.

In view of above, this work is an attempt to develop a polymer matrix composite which can behave as appropriate dielectric as well as conducting material depending on vol %/wt % of filler content. As host polymer matrix, polycarbonate (PC) was selected due to its good dimensional and dielectric stability over wide range of temperature ($-55°C$ to $125°C$), highest toughness among engineering thermoplastics, good tensile strength (65 MPa), good creep resistance, negligible moisture absorption, and resistance to oils and chemicals.[23] In this work, as conducting filler, few layer graphene (FLG), prepared by dry ice method, has been used. It is also good to use carbonaceous filler due to its low density (comparable to polymers) which finally results in flexible and light weight composite. The sheet morphology of FLG (instead of fibrous morphology in case of carbon nanotubes) is expected to increase the smearing range in which the dielectric constant can be improved.

EXPERIMENTAL

Polycarbonate in the form of granules was used as matrix material. FLG was used as conducting filler. It was prepared using dry ice method as suggested by Chakrabarti et al.[24] and is discussed in the coming section. Solution mixing method was used to prepare nanocomposites. Tetrahydrofuran (THF) was used as solvent for solution mixing. The details of composite preparation are given elsewhere.[25,26] Nanocomposite samples containing 1, 2, 3.5, 5, 6, and 7 wt % of FLG in the PC matrix were prepared (2 samples for each composition). X-ray diffraction (XRD) (X'Pert PRO PANalytical) and Raman Spectrometer (STR300, Laser: 532 nm), Transmission electron microscopy (FEI: TECNAI G^2, operated at 200 kV), Scanning electron microscopty (FEI: NovaNano SEM-450) were employed to characterize the samples. Dielectric properties and electronic conductivity of the composites were evaluated using a Wayne Kerr Electronics precision impedance analyzer (6515B, UK). The dielectric constant and conductivity of the composites were determined using the formula given in eqs. (1) and (2), respectively.

$$\varepsilon = C.t/\varepsilon_o.S \tag{1}$$

$$\sigma = 1/[Z.S/t] \tag{2}$$

where, ε is the permittivity of the sample, C is the capacitance, σ is the conductivity, ε_o (8.854×10^{-12} F/m) is the permittivity of free space, Z is the impedance, S is the surface area, and t is the thickness of the sample. The dissipation factor was directly measured from the instrument.

Preparation Method of Few-Layer-Graphene (FLG)

Magnesium ribbon of 99% purity, obtained from local market in Jaipur, was used to prepare graphene. A bowl was prepared from the dry ice (Solid carbon dioxide). Totally, 3 g of Mg ribbon was put in this bowl and ignited with the help of burner. The bowl was immediately covered with another dry ice bowl. The following reaction as given in eq. (3) was involved during the combustion process.

$$2Mg(s) + CO_2(g) \rightarrow 2MgO(s) + C(s) \tag{3}$$

After the complete combustion of Mg, a black colour carbonaceous product was obtained and is collected in a beaker. The carbonaceous product was likely to contain MgO and unburned Mg as impurities. To remove these undesirable traces of impurities, the black product was stirred overnight in 100 mL of $1M$ Hydrochloric acid. Both MgO and Mg form $MgCl_2$ when react with HCl. $MgCl_2$ is soluble in water. The mixture was filtered and washed several times with deionized water until the filtrate attained neutral pH. The final solid carbonaceous product was then dried in vacuum oven at $100°C$ for 18 h. The carbonaceous product was analyzed by a combination of XRD, Raman spectroscopy and TEM. The product was confirmed to be few layer graphene (FLG).

RESULTS AND DISCUSSION

Characterization

The FLG, prepared in the laboratory was characterized using a combination of X-ray diffractometry (XRD), Raman spectroscopy and transmission electron microscopy (TEM). X-ray
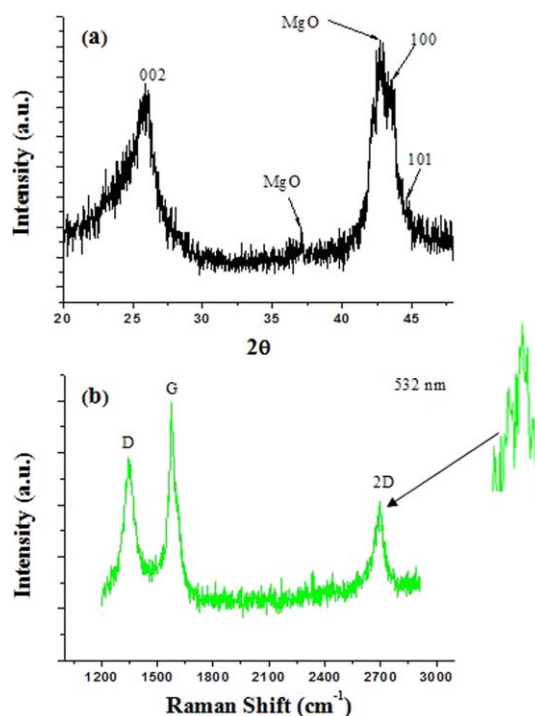

Figure 1. (a) The XRD pattern of FLG sample, (b) The Raman spectrum of FLG; favoring few-layer-graphene in the sample. [Color figure can be viewed in the online issue, which is available at wileyonlinelibrary.com.]
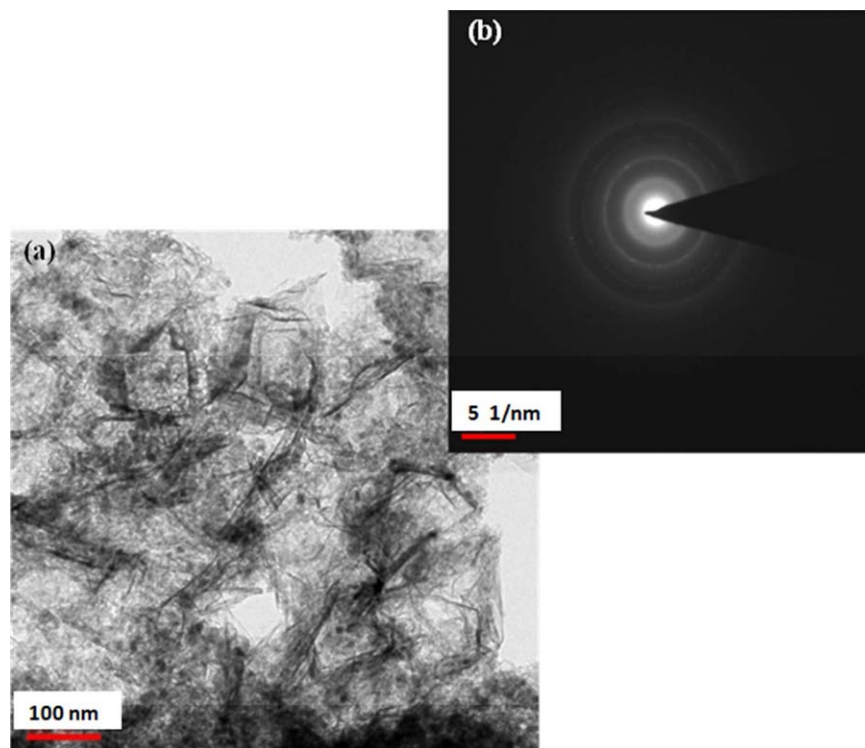
Figure 2. (a) The TEM image of FLG sample (b) The electron diffraction pattern taken from a FLG sheet. [Color figure can be viewed in the online issue, which is available at wileyonlinelibrary.com.]

diffraction pattern of the FLG is shown in Figure 1(a). The presence of MgO as impurity is apparent from the peaks in XRD trace. The prominent (002) peak from graphene, at 26.2°, is observed along with the (101) peak at 44.6°. The other characteristic peak for graphene structure is (100) peak located at about 43.3°. The Raman spectrum of FLG is shown in Figure 1(b). Observed Raman spectrum confirms the presence of single sharp 2D band at 2700 cm^{-1} which provides strong evidence in favour of graphene. The splitting of 2D band peak confirms the graphene to be few layered. The presence of D band at about 1350 cm^{-1} is due to the disorder in the graphene. The above characterization data for FLG are in support with the finding of Chakrabarti et al.[24]

TEM image of FLG sample is shown in Figure 2(a). It can be seen that FLG has sheet like morphology. Presence of some impurities is also evident in this image. Figure 2(b) is the electron diffraction (ED) pattern taken from an individual graphene layer. The ED pattern is favoring the reflection from hexagonal crystal structure of graphene. The relatively sharp rings should be indicative of amorphous carbon layer on the copper grid, because the electron beam might penetrate the thin graphene sheet.

Figure 3(a,b) show the TEM images of a FLG/PC composite at different locations and magnifications. Figure 3(c) is the ED pattern taken on an FLG sheet embedded in PC matrix. The ED pattern favouring the hexagonal structure, but the reflection is coming from the different layers having different crystal orientation. Such type of ED pattern for graphene filled polymer composite has also been reported in a previous work of Stankovich

et al.[27] Figure 4(a,b) are the SEM views of polished and fractured surface (cross sectional), respectively of FLG(5 wt %)/PC - nanocomposite. The FLG sheets are well distributed and making connections with each others.

XRD trace in Figure 5 confirms the presence of FLG in the PC matrix. The XRD traces from PC show broad peak at about 17°. It was found that the halo-reflection was somewhat sharper and narrower in controlled PC (treated with THF) and FLG/PC nanocomposite than it was in case of as-received PC. While solution treating with THF, the polymer chains are separated with negligible connections in between them. As the solvent starts to evaporate the concentration increases and chains start to interact with each other favouring the crystallization to some extent. Works by Schorn et al.[29] and Lehmann[30] strongly favor the crystallization from solution. Furthermore, the presence of nanofiller (here FLG) may work as nucleation site for polymer and may increase the crystallites embedded in amorphous region. Hence, in controlled PC and FLG/PC nanocomposite, due to increased crystallized domains, the polymer chains were more orderly attached than attached in as-received PC, resulted in the narrower and sharper peak. A peak near about 73° was present in all the XRD traces and was due to the sample holder as shown in inset in Figure 5, hence should be ignored in all the cases. In the XRD pattern of FLG (5 wt %)/PC, the (002) peak along with (101) peak is apparent. Other peaks were also found which should be due to MgO impurity.

Electrical Behavior of the System

AC Conductivity. AC electrical conductivity of the FLG/PC nanocomposite system was measured and plotted as a function
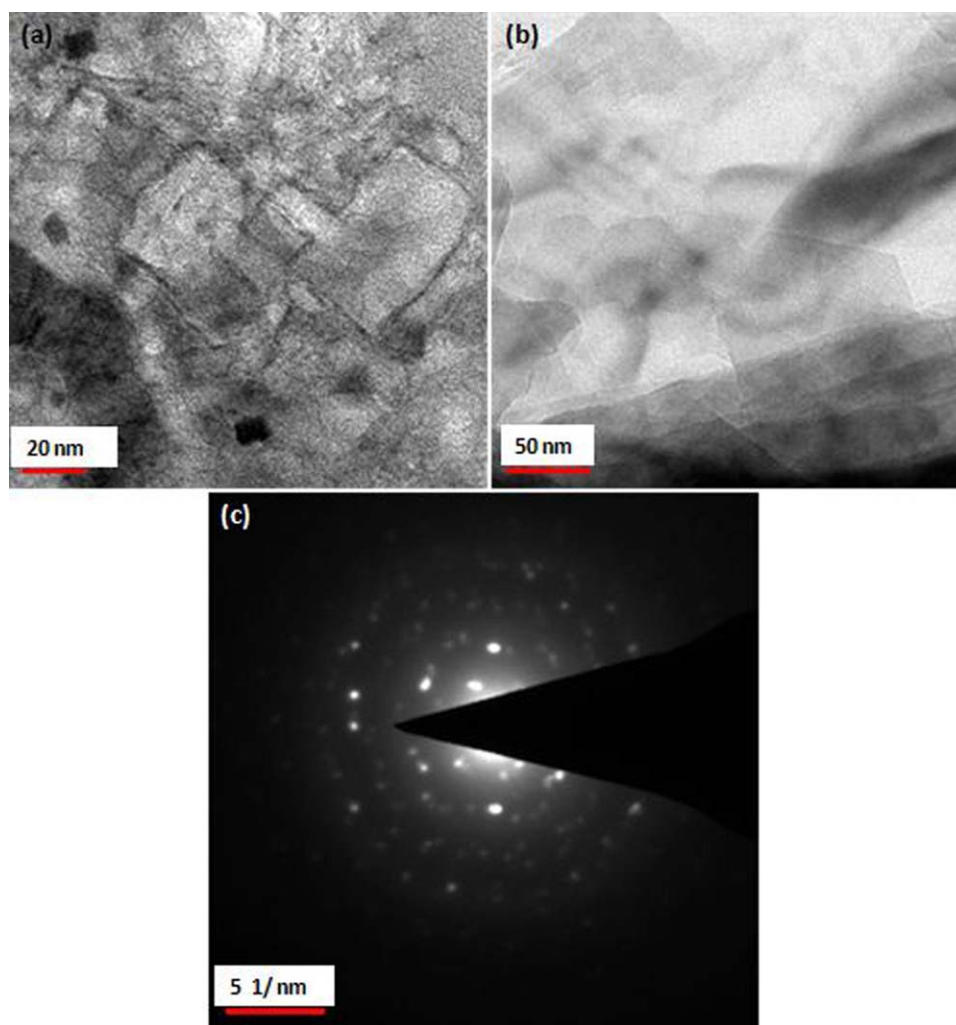
Figure 3. TEM micrographs of (a) FLG (5 wt %)/PC nanocomposite (b) FLG(5 wt %)/PC at thinner section; showing good dispersion of FLG in PC matrix, (c) ED pattern taken from FLG sheet embedded in PC matrix. [Color figure can be viewed in the online issue, which is available at wileyonlinelibrary.com.]

of FLG wt %. Figure 6 shows the electrical conductivity of the composite system as a function of FLG weight percent. It can be observed that as the FLG wt % increased, the conductivity remained almost constant up to 3.5 wt %. Below 3.5%, the FLG layers are seemed to be well separated by the polycarbonate and there was no interaction at all in between the FLG layers. The conductivity will jump abruptly if somehow the electric charges start to transport. The freely available charges in graphene layers can not cross the thick insulating layer of polycarbonate. Beyond 3.5%, the conductivity started to increase abruptly, indicating that beyond this level, the FLG layers started to interact with each other. The interaction may be due to quantum tunnelling of the charge carriers or may be due to physical contact in between the adjacent FLGs. At some level, the charge carrier can tunnel from one conducting layer to another adjacent conducting layer through the thin insulating layer, before physical contact. The system, in which the quantum tunnelling takes place is expected to show a wide range of transition region (smearing range) or may show double percolation (second, when filler physically interact). The concept for movement of

charge carriers due to tunnelling can be found in previous works also.[16,17,28] According to the concept when the thickness of the insulating polymer in between conductive fillers becomes comparable to the wavelength of the electron, the electron can tunnel and hope to the adjacent conducting filler. The probability of the tunnelling may be very low and hence one can say the quantum tunnelling does not provide easy path to charge carriers to flow throughout the system, but locally reduces barrier potential in between the adjacent conductive fillers; hence locally, the movement of the charge carrier becomes flexible. Local flexibility in the movement of charge increased the conductivity level of the composite (conductivity at 5 wt %). Beyond 5% the conductivity again increased with higher rate (can be refer to second percolation), which should be due to the physical contact of the FLG layers. It can be concluded that in the studied system the percolation onsets at 3.5 wt % and smearing range is up to 6 wt % (i.e., smearing range is from 3.5 to 6 wt %). The conductivity, between 6 and 7 wt % of FLG, increased at much slower rate than that in smearing region.
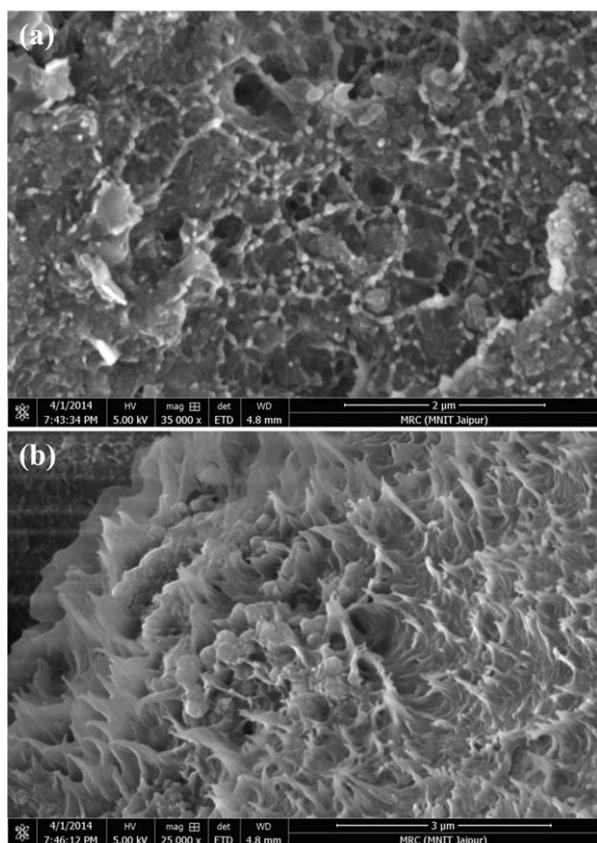
Figure 4. The SEM images of (a) polished surface, (b) fractured surface of the FLG(5 wt %)/PC nanocomposite.

Dielectric Constant and Dissipation Factor. The dielectric constant is also evaluated and plotted as a function of FLG wt %. It was found that the dielectric constant increases with the same trend as observed for conductivity, as apparent in Figure 7. In
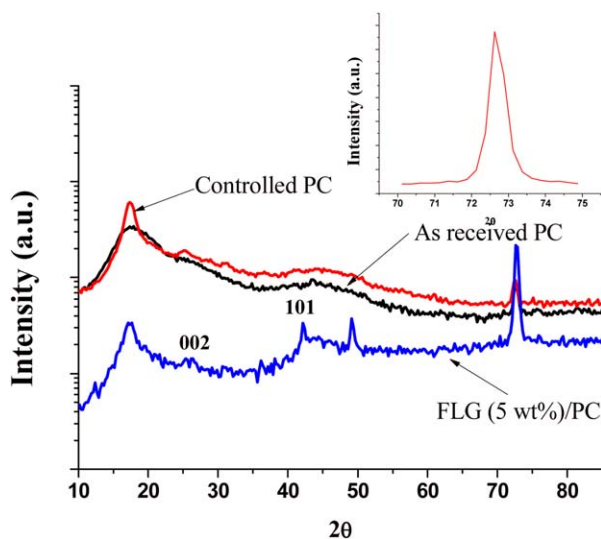

Figure 5. XRD patterns of as-received PC, controlled PC and FLG (5 wt %)/PC nanocomposite. The inset figure is showing the XRD trace of sample holder. [Color figure can be viewed in the online issue, which is available at wileyonlinelibrary.com.]
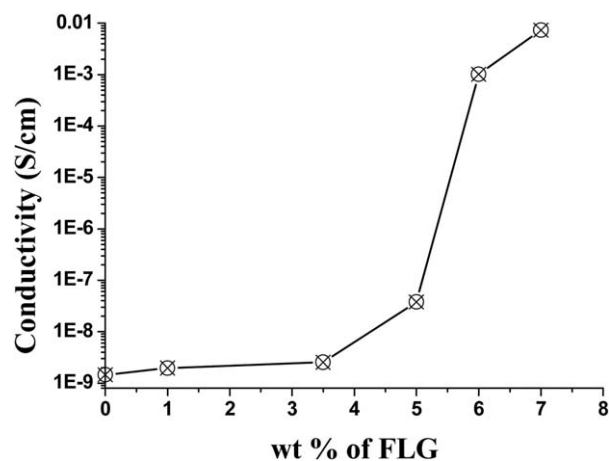

Figure 6. The AC conductivity of the FLG/PC system measured at 1 kHz, as a function of FLG wt %.

the smearing region the augment in the dielectric constant was reported up to about 70 with 0.07 dissipation factor (at 5 wt %). This is a good achievement for polycarbonate based dielectrics from the application point of view in embedded capacitor technology. The abrupt increment in the dielectric constant in the smearing region should be due to the local quantum tunnelling of charge carriers through thin insulating polymer layer. Due to this quantum tunnelling the charge can displace easily and can store energy in the form of electrostatic energy in the composite. With such scenario, the conducting FLG layers are separated by thin insulating layer and each tiny set of FLG-polymer-FLG works as a micro-capacitor. The complete composite system possesses a large number of micro-capacitors. The capacitance contributed by each of these micro-capacitors can be correlated with the abrupt increment in the dielectric constant of the composite system. The sheet shape of the FLG provides large surface area which also favors higher capacitance of each micro-capacitor in the composite.

Frequency Dependence of Dielectric Constant and Dissipation Factor. The stability of the dielectric constant was also analysed within 1 kHz to 1 MHz frequency range. Figure 8 shows
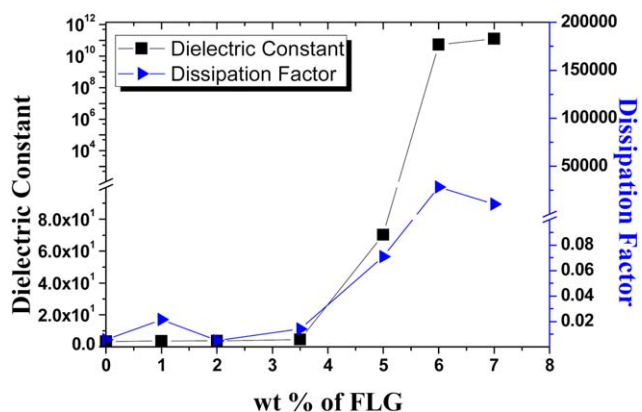

Figure 7. The dielectric constant and dissipation factor as a function of FLG wt %, at 1 kHz. [Color figure can be viewed in the online issue, which is available at wileyonlinelibrary.com.]
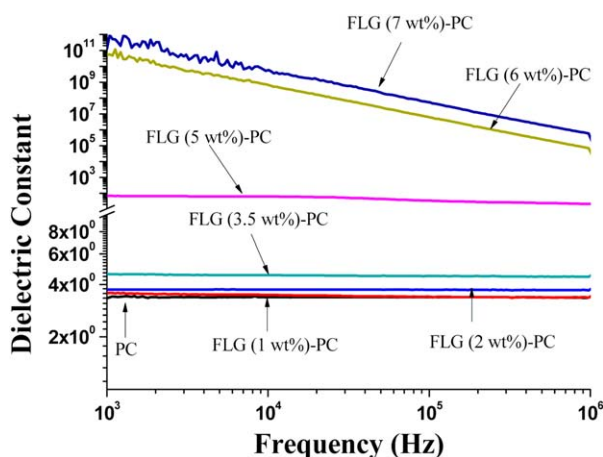
Figure 8. Variation in the dielectric constant of FLG/PC nanocomposites as a function of frequency. [Color figure can be viewed in the online issue, which is available at wileyonlinelibrary.com.]

the dielectric constant as a function of frequency. The dielectric constant is almost constant within the studied frequency range up to 3.5 wt % loading of FLG. However, at high frequency end the slight decrease was observed which is due to the mismatch of polarisation relaxation time with the frequency of electric field at high frequencies. Beyond 5 wt %, the dielectric constant decreases with increasing frequency. At lower frequencies the higher value of dielectric constant is due to the large Maxwell-Wagner-Sillars polarization[9,31] at the interface of FLG and PC which results in increased free space charges. The interfacial polarization becomes less and less dominant with increasing frequency and hence the dielectric constant of the composites decreased with increasing frequency.

Figure 9 shows the frequency dependence of the dissipation factor. As the frequency increases, due to the mismatching of relaxation time of particular polarization mechanism and field frequency, the loss factor increases, hence the dissipation factor showed slight increasing trend with increasing frequency. Beyond percolation, when the system became percolative, the
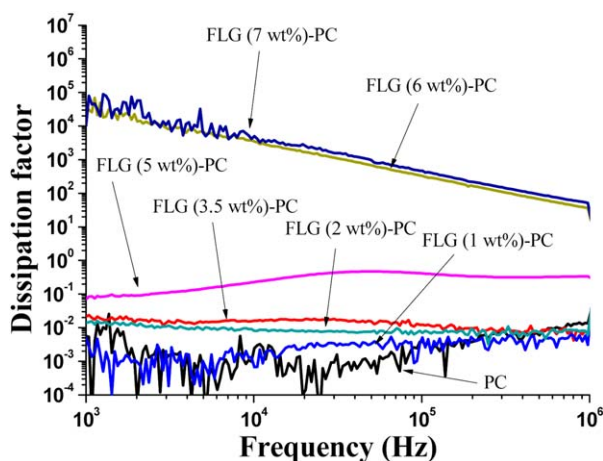

Figure 9. Variation in the dissipation factor of FLG/PC nanocomposites as a function of frequency. [Color figure can be viewed in the online issue, which is available at wileyonlinelibrary.com.]

rapid drop in the dielectric constant must be attributed to the large leakage current which also gives rise to high dissipation factor which is the feature of percolative systems.[32]

CONCLUSIONS

The FLG/PC nanocomposite system has been prepared successfully with sufficiently wide smearing range. The percolation threshold in the system found to occur at 3.5 wt % of FLG. The nanocomposite exhibited double percolation. In the smearing range the dielectric constant was increased considerably to almost 20 times (from 3.37 to 70) with dissipation factor of 0.07 which is near to the tolerance limit for most of dielectric applications. The conductivity level of 0.01 S/cm was achieved at 7 wt % of FLG. The prepared system is supposed to be a versatile nanocomposite system with application point of view. Based on the above findings, it is suggested that polycarbonate-based nanocomposite system could be a potential dielectric material below percolation (for instance, in embedded capacitor technology) and can be a conducting polymeric composite material beyond percolation (for instance, in electromagnetic shielding applications).

REFERENCES

1. Yoon, J. R; Han, J. W.; Lee, K. M. *Trans. Elect. Electro. Mater.* **2009**, *10*, 116.

2. Xu, J.; Wong, C. P. *J. Electr. Mater.* **2006**, *35*, 1087.

3. Singh, V.; Kulkarni, A. R.; Rama Mohan, T. R. *J. Appl. Poly. Sci.* **2003**, *90*, 3602.

4. Qureshi, A.; Mergen, A.; Eroglu, M. S.; Singh, N. L.; Gulluoglu, A. *J. Macro. Sci. A: Pure Appl. Chem.* **2008**, *45*, 462.

5. Li, Y. J.; Xu, M.; Feng, J. Q.; Dang, Z. M. *Appl. Phy. Lett.* **2006**, *89*, 1.

6. Lim, E. S.; Lee, J. C.; Kim, J. J.; Park, E. T.; Chung, Y. K.; Lee, H. Y. *Int. Ferro.* **2005**, *74*, 53.

7. Dai, L. 2004, Chapter 2-Conducting Polymers, Springer, 74.

8. Kulthe, M. G.; Goyal, R. K. *Adv. Mater. Lett.* **2012**, *3*, 246.

9. Goyal, R. K.; Kadam, A. *Adv. Mater. Lett.* **2010**, *1*, 143.

10. Xu, J.; Wong, M.; Wong, C. P. Electronic Component and Technology Conference, *IEEE.* **2004**, *536*.

11. Carmona, F. *Physica A* **1984**, *157*, 461.

12. Boudenne, A.; Ibos, L.; Fois, M.; Majeste, J. C.; Gehin, E. *Compos. A* **2005**, *36*, 1545.

13. Mamunya, Y. P.; Davydenko, V. V.; Pissis, P.; Lebedev, E. V. *Euro. Poly. J.* **2002**, *38*, 1887.

14. Luyt, A. S.; Molefi, J. A.; Krump, H. *Polym. Degrad. Stab.* **2006**, *91*, 1629.

15. Balberg, I. *Phy. Rev. Lett.* **1987**, *59*, 105.

16. Psarras, G. C. *Compos. A* **2006**, *37*, 1545.

17. Nan, C. W.; Shen, Y.; Ma, J. *Annu. Rev. Mater. Res.* **2010**, *40*, 131.

18. George, S.; Sebastian, M. T. *Compo. Sci. Tech.* **2009**, *69*, 1298.

19. Yao, S. H.; Dang, Z. M.; Jiang, M. J.; Xu, H. P.; Bai, J. *Appl. Phy. Lett.* **2007**, *91*, 212901.

20. Eken, A. E.; Tozzi, E. J.; Klingenberg, D. J.; Bauhofer, W. *J. Appl. Phy.* **2011**, *109*, 084342.

21. Moreno, I.; Navascues, N.; Irusta, S.; Santamaría, J. *IOP Conf. Series: Mater. Sci. Eng.* **2012**, *40*, 012001.

22. Boudenne, A.; Ibos, L.; Fois, M.; Majeste, J.; Gehin, E. *Compos. A* **2005**, *36*, 1545.

23. Bhargava, A. K. Engineering Materials: Polymers, Ceramics and Composites (New Delhi: PHI Learning), 111, **2012**.

24. Chakrabarti, A.; Lu, J.; Skrabutenas, J. C.; Xu, T.; Xiao, Z.; Maguire, J. A.; Hosmane, N. S. *J. Mater. Chem.* **2011**, *21*, 9491.

25. Sain, P. K.; Goyal, R. K.; Bhargava, A. K.; Prasad, Y. V. S. S. *J. Appl. Polym. Sci.* **2014**, *131*, 39913.

26. Sain, P. K.; Goyal, R. K.; Bhargava, A. K.; Prasad, Y. V. S. S. *J. Phys. D. Appl. Phys.* **2013**, *46*, 455501.

27. Stankovich, S.; Dikin, D. A.; Dommett, G. H. B.; Kohlhaas, K. M.; Zimney, E. J.; Stach, E. A.; Piner, R. D.; Nguyen, S. T.; Ruoff, R. S. *Nat. Lett.* **2006**, *442*, 282.

28. Arjmand, M.; Mahmoodi, M.; Gelves, G. A.; Park, S.; Sundararaj, U. *Carbon* **2011**, *49*, 3430.

29. Schorn, H.; He, B.; Kosfeld, R. In Integration of Fundamental Polymer Science and Technology-2; Lemstra, P. J.; Kleintjens, L. A., Eds., **1988**; p 385.

30. Lehmann, J. *Colloid Polym. Sci.* **1966**, *212*, 167.

31. Yousefi, N.; Sun, X.; Lin, S.; Shen, X.; Jia, J.; Zhang, B.; Tang, B.; Chan, M.; Kim, J. K. *Adv. Mater.* **2014**, *26*, 5480.

32. Li, Y. J.; Xu, M.; Feng, J. Q. *Appl. Phys. Lett.* **2006**, *89*, 072902.